Journal Pre-proof

Water softening using graphene oxide/biopolymer hybrid nanomaterials

Luciana S. Rocha, João Nogueira, Ana Luísa Daniel-da-Silva, Paula Marques, Sara Fateixa, Eduarda Pereira, Tito Trindade

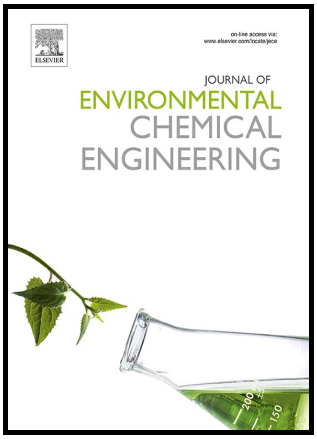

PII: S2213-3437(21)00023-3

DOI: https://doi.org/10.1016/j.jece.2021.105045

Reference: JECE105045

To appear in: *Journal of Environmental Chemical Engineering*

Received date: 14 October 2020
Revised date: 17 December 2020
Accepted date: 6 January 2021

Please cite this article as: Luciana S. Rocha, João Nogueira, Ana Luísa Daniel-da-Silva, Paula Marques, Sara Fateixa, Eduarda Pereira and Tito Trindade, Water softening using graphene oxide/biopolymer hybrid nanomaterials, *Journal of Environmental Chemical Engineering,* (2020) doi:https://doi.org/10.1016/j.jece.2021.105045

This is a PDF file of an article that has undergone enhancements after acceptance, such as the addition of a cover page and metadata, and formatting for readability, but it is not yet the definitive version of record. This version will undergo additional copyediting, typesetting and review before it is published in its final form, but we are providing this version to give early visibility of the article. Please note that, during the production process, errors may be discovered which could affect the content, and all legal disclaimers that apply to the journal pertain.

© 2020 Published by Elsevier.

Journal Pre-proof

Water softening using graphene oxide/biopolymer hybrid nanomaterials

Luciana S. Rocha[1], João Nogueira[1], Ana Luísa Daniel-da-Silva[1*], Paula Marques[2], Sara Fateixa[1], Eduarda Pereira[3] & Tito Trindade[1]

[1] CICECO and Department of Chemistry, University of Aveiro, 3810-193 Aveiro, Portugal.

[2] TEMA-NRD, Mechanical Engineering Department, University of Aveiro, 3810-193 Aveiro, Portugal

[3] LAQV-REQUIMTE & CESAM, Department of Chemistry, University of Aveiro, 3810-193 Aveiro, Portugal.

Journal Pre-proof

Abstract

There is a growing interest in developing more environmentally friendly softeners for hardness reduction of water supplied for domestic consumption. This work focuses on exploring biopolymer-based softeners, through the surface modification of graphene oxide (GO) with the anionic biopolymer κ-carrageenan (GO-Si(κ)CRG). The performance of the modified GO to decrease the hardness of natural waters containing high levels of Ca^{2+} was assessed. The sorption efficiency was dependent on the initial Ca^{2+} concentration and on the sorbent dose, with 8-34% removal for GO and 21-100% for GO-Si(κ)CRG. The surface modification considerably improved the adsorptive efficiency and under certain experimental conditions, it was possible to convert very hard water (300 mg L^{-1} $CaCO_3$) to soft water. Importantly, the performance was not affected by the presence of other ions typically found in natural bottled waters. The kinetics was well described by pseudo-first-order and diffusion models. The multi-linear nature observed in Boyd's and Webber's plots suggested that both film diffusion and pore diffusion controlled the sorption rate. The maximum Ca^{2+} sorption capacity at monolayer coverage of GO-Si(κ)CRG was 47.6±3.2mg g^{-1}. The electrostatic attraction between sulfonate groups and calcium cations is likely to be the main mechanism involved in the sorption process of Ca^{2+} by GO-Si(κ)CRG. Overall, the results indicate

good prospects for the development of a new class of softeners based on the GO modification described.

Keywords: Water hardness; Graphene oxide; polysaccharide; Softeners; Water treatment.

1. INTRODUCTION

The presence of high levels of calcium and magnesium ions in water supplies are responsible for causing hard scale problems in residential settings [1,2]. The combination of these cations with carbonate, sulfate or phosphate anions leads to the formation of precipitates that can cause film and scale buildup in plumbing, fixtures, and appliances, affecting their performance, increasing the energy costs and the effectiveness of most cleaning tasks. Therefore, the degree of hardness of drinking-water is important for both economical and operational concerns, and for safety reasons. Hardness is caused mainly by the presence of dissolved Ca^{2+} and Mg^{2+}, however other polyvalent metallic cations, namely aluminum (Al), barium (Ba), iron (Fe), manganese (Mn), strontium (Sr) and zinc (Zn), have a small contribution to water hardness [3,4]. Due to the levels of Ca found in natural water sources (up to and exceeding 100 mg L^{-1}), calcium-based hardness usually predominates [4]. Hardness is typically expressed as milligrams of calcium carbonate ($CaCO_3$) equivalent per liter, and according to the guidelines for drinking water quality established by the World Health Organization (WHO), water can be classified as: 1) soft, for $CaCO_3$ at concentrations below 60 mg L^{-1}; 2) moderately hard when the values range between 60–120 mg L^{-1}, 3) hard for 120–180 mg L^{-1} and 4) very hard for values higher than 180 mg L^{-1} [4].

Water softening (i.e. hardness decrease) is an effective method to reduce the levels of Ca, Mg and other hard ions (e.g. Fe and Mn), and has been practiced in a wide

variety of installations (e.g. chemical industries, power plants, laundries, individual households, and drinking water treatment plants) [5]. Softening water methods are normally based on chemical and thermochemical methods, reverse osmosis and ion exchange processes [3,6]. Despite their efficiency, these methods imply significant costs of energy, resources and/or excessive use of chemicals, leading in some cases to secondary waste disposal problems [2,7,8]. Ion-exchange polymeric resins have been commonly used in households to decrease water hardness. In this case, the ion-exchange process involves the substitution of both dissolved Ca^{2+} and Mg^{2+} ions typically by Na^{+}, supplied by dissolved NaCl salt or brine employed in the resin regeneration. The frequent release of concentrated brine from ion exchange softeners has been identified as an environmental problem, contributing to the contamination of freshwater supplies. Indeed, some countries have already implemented strict legislation regarding the use of ion exchange water softeners [1]. On the other hand, NaCl that remains in softened water (from a conventional water softener) for human consumption can be a health problem for those on sodium-restricted diets [8]. Thus, there is a need for more ecological and friendly alternative methods and/or materials for water softening. The use of sorption materials has been proposed as a cost-effective and environmentally friendly technology in water softening [7,9–13].

Graphene oxide (GO) is a derivative of the highly valued graphene and is composed of planar graphene-like aromatic domains (sp^2) of random size separated by sp^3-hybridized carbons, displaying hydroxyl, epoxy, and carboxyl groups. Due to its similarities with graphene, GO preserves many of its properties, but it is much simpler and less expensive to obtain in large quantities and also easier to process [14]. The presence of oxygen functional groups make GO sheets strongly hydrophilic and highly

dispersible in water and polar organic solvents, which ensures a broad coverage for the conception and application of GO composite materials [15,16]. The negatively charged nature and the presence of oxygen groups on GO surface, favors a vast range of chemical interactions with molecules or ions. Furthermore, it allows further chemical modification to introduce novel functionalities. The application of neat GO membranes in water softening processes [17] and the ability of graphene-based materials to adsorb metallic trace metals [14,18,19] and dyes [20] has already been reported. Besides that, one of the interesting features of using GO is the possibility of obtaining flexible GO nanosheets with a foam-like structure and this morphology could favour the contact with water [21] and open the possibility for real commercial applications. Herein, we have explored a new route to develop biopolymer-based sorbents to remove Ca^{2+} and other hard ions from hard waters by modifying the surface of GO with the polysaccharide κ-carrageenan (κ-CRG). κ-Carrageenan is a natural linear water-soluble polysaccharide extracted from red seaweeds that contains sulfonate ($–OSO_3^-$) groups in its backbone. Due to its environmental-friendly, biodegradability, and non-toxicity properties, this biopolymer has been applied in the development of composite materials for water treatment [22,23]. Previously, Yang *et al.* synthesized gel beads of κ-carrageenan biopolymer physically adsorbed on GO by a simple method and explored its adsorption capacity towards the removal of methylene blue organic dye from aqueous solutions [20]. Hefnawy *et al.* evaluate the performance of GO gel beads modified with carboxymethylcellulose and κ-CRG towards the removal of copper and cobalt ions from aqueous solutions [24]. The surface modification proposed in this work is expected to improve the stability of GO chemically modified through grafting with κ-CRG (GO-Si(κ)CRG) and also to enhance the adsorptive capacities in the new hybrid materials, as

compared to neat GO, due to extensive presence of Lewis bases namely as sulfonate groups from the biopolymer. κ-carrageenan has been successfully employed in previous studies in the functionalization of colloidal magnetic nanoparticles for the removal of organic pollutants in water, where the negatively charged sulfonate groups of the polymer reliably interact with positively charged pollutant molecules via electrostatic interactions [25–27].

In this work, metal cations dissolved in water are the target sorbates, as such, a biopolymer which is negatively charged across most of the pH range was selected to improve the GO's sorption properties. Furthermore, κ-carrageenan is a polysaccharide of natural origin, which is in line with the aim of developing environmentally friendly softeners. Therefore, the performance of bare and modified GO in the removal of Ca^{2+} from aqueous media was evaluated and the influence of different parameters affecting the sorption process were assessed, together with the kinetic and equilibrium studies. To accomplish these goals and to address some of the gaps of the studies reported in the literature, namely the lack of information regarding the competition of other ions available in natural waters, all adsorption experiments were conducted in bottled waters, spiked with realistic Ca^{2+} concentrations.

2. MATERIALS AND METHODS

2.1. Reagents

All chemicals used were of analytical reagent grade. Calcium and potassium chloride salts ($CaCl_2.2H_2O$ and KCl) and 1000 ppm $Ca(NO_3)_2$ standards were purchased from Merck. A GO water dispersion (0.4 wt %, 4 mg mL^{-1}) was purchased from Graphenea and according with the product specifications, the monolayer flakes of GO

were obtained by chemical processing of graphite and subjected to a rigorous quality control to ensure high quality and reproducibility. The biopolymer κ-CRG (MW 300,000 g mol^{-1}) was obtained from Fluka Chemie. 3-isocyanatopropyltriethoxysilane (ICPTES, 95%), tetraethyl orthosilicate (TEOS, 99%) and triethylamine were purchased from Sigma–Aldrich. Dimethylformamide (DMF) was obtained from Carlo Erba Reagents and ammonia (25%) was from Riedel-de-Häen. Ethanol and methanol (>99%) were purchased from Panreac and VWR, respectively. Biohit Proline pipettes equipped with disposable tips were used for appropriate dilutions. All glassware material used in the experiments was acid washed prior use. Solutions were prepared in ultrapure water (18.3 MΩ cm, Milli-Q systems, Millipore-waters) or commercial bottled water for Ca^{2+} or Ca^{2+}/Mg^{2+} solutions used in the sorption experiments

2.2. Synthesis of biopolymer–GO hybrid

The biopolymer–GO hybrid nanomaterial was prepared from GO sheets and the biopolymer κ-CRG, by using a two-step procedure. In the first step an alkoxysilane derivative of carrageenan, Si(κ)CRG, was synthesized through the reaction of ICPTES with the polysaccharide κ-CRG. The isocyanate group of ICPTES reacts with hydroxyl groups of κ-CRG to form a urethane bond (Scheme S1, supplementary material). The reaction was conducted in the aprotic solvent DMF under an inert (N_2) dry atmosphere to ensure that the isocyanate groups reacted only with the OH groups of the polysaccharide. The reaction was maintained for 24 h, at 100ºC, under constant stirring. The Si(κ)CRG precursor was then collected by centrifugation, washed first with dry methanol (8 times), then washed twice with dry ethanol, and finally dried in an oven (40 ºC) [28]. In the second step the hybrid GO-Si(κ)CRG was prepared by adding 13.3 mL of

a GO suspension (4 mg mL^{-1}) to 6.7 mL of ultrapure water. After that, 0.3 g of Si(κ)CRG were dispersed in a mixture of TEOS (0.4 mL) and ethanol (3 mL), and the mixture was added to the GO suspension. The reaction started with the addition of 0.1 mL of triethylamine and took place in an ice bath, under sonication and for 25 minutes. The resulting material was washed thoroughly with ethanol, twice with ultrapure water and finally freeze-dried. The material produced was characterized by its spongy appearance. Scheme 1 presents the chemical route regarding the grafting process of GO with the alkoxide derivative of the biopolymer κ-carrageenan (Si(κ)CRG).

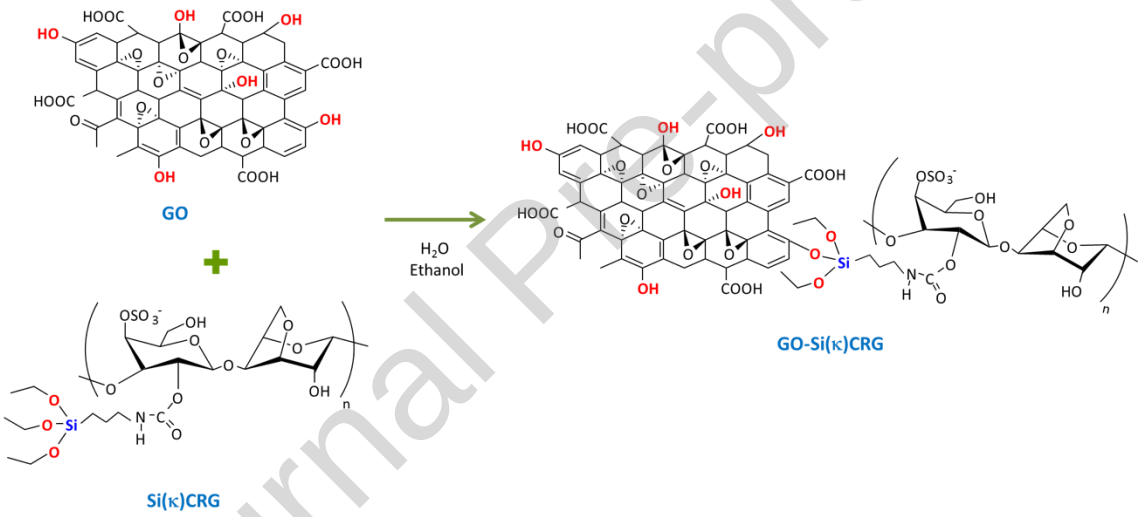

Scheme 1. Schematic of modification of GO (Dimiev–Alemany–Tour model [29]) with Si(κ)CRG.

2.3. Characterization of GO and GO-Si(κ)CRG nanomaterials

The carbon, hydrogen, nitrogen and sulphur contents, expressed in weight percentage, were determined for the GO, Si(κ)CRG and GO-Si(κ)CRG nanomaterials. The analysis was performed using a LecoTruspec Micro CHNS Analyzer Model 630-200-200, with a sample size of 2 mg, combustion furnace temperature of 1075 ºC, after

burner temperature of 850 ºC and detection method of infrared absorption for carbon, hydrogen and sulphur, and thermal conductivity for nitrogen.

The functional groups present in GO, Si(κ)CRG and GO-Si(κ)CRG were characterized by Fourier transform infrared (FT-IR) spectroscopy, using a Bruker Optics Tensor 27 spectrometer (Billerica, MA, USA) coupled to a horizontal attenuated total reflectance (ATR) cell, using 128 scans at a 4 cm^{-1}resolution and Raman spectroscopy, using a combined Raman-AFM confocal microscope WITec alpha300 RAS+. A Nd:YAG laser operating at 532 nm was used as excitation source with the power set at 1 mW (2 s,10 acquisitions each spectrum).

The surface areas of both GO and GO-Si(κ)CRG nanomaterials were examined by gas adsorption using a Gemini V-2380 surface area analyser (Micromeritics, Norcross, GA, USA). Prior to the measurements, the samples were degassed overnight at 100 ºC. The pore volume (V_p) was determined through the BJH (Barrett-Joyner-Halenda) model and the specific surface area (S_{BET}) was determined using the Brunaer–Emmett–Teller (BET) equation with multipoint adsorption isotherms of N_2 at -196 ºC.

Zeta potential measurements were performed using a Zetasizer Nano ZS from Malvern Instruments (Malvern, United Kingdom). For these measurements GO and GO-Si(κ)CRG materials were first crushed and then dispersed in water. To assure the formation of a homogeneous dispersion, the solutions were sonicated for 1 minute prior to the measurement of zeta potential. The pH of the solution was adjusted with 0.1 mol L^{-1} HCl or 0.1 mol L^{-1} NaOH solutions.

The morphological features of the hybrid materials were evaluated by scanning electron microscopy (SEM) using a Hitachi Su-70 (Hitachi, Tokyo, Japan) equipment operated at an accelerating voltage of 15 kV.

2.4. Characterization of bottled water

Bottled water Serra da Estrela is commercialized in Portugal, being derived from Cabeça do Velho, Paços da Serra, Gouveia, Portugal (40º25'51.967''N7º36'22.842''W). Prior to its use, the water sample was characterized in terms of pH, conductivity and concentration of Ca, Mg and other major and minor elements. The aqueous solutions containing Ca^{2+} or Ca^{2+} and Mg^{2+} and used in the sorption studies, were prepared using bottled water. By using a naturally occurring water enriched with a controlled concentration of Ca^{2+}, the impact of other cations and anions in real water matrices will be evaluated. Therefore, it is possible to mimic the water matrix used in softening processes and guarantee a control in water parameters (pH, conductivity, and concentration of minor and major ions).

2.5. Batch adsorption studies

In order to evaluate the sorption efficiency of GO and GO-Si(κ)CRG nanomaterials in the removal of Ca^{2+} from water, isothermal batch experiments were carried out (21±2°C). The experiments were performed in 50 mL falcon tubes, keeping the materials in contact with a known concentration of Ca^{2+}, under constant stirring conditions (150 rpm), and monitoring the concentration of this cation in solution over time. The tested initial concentrations of Ca^{2+} ($C_{Ca,0}$) were 30 and 120 mg L^{-1} and the aqueous solutions were prepared in bottled water. In these experiments, the amount of

sorbent used per unit volume of solution (m/V) was varied between 0.25 and 10 g L^{-1}. The pH of the solutions was kept between 6.8 and 7.2 (without pH adjustments). Experiments without GO and GO-Si(κ)CRG (control) were run in parallel in order to quantify the concentration of Ca^{2+} (or other ions) in spiked bottled water and to assess the losses and or contaminations of Ca^{2+} during the experimental runs (always inferior to 5%). The experiments started when the respective sorbent material was added to the Ca^{2+} solutions and stirring was initiated. Aliquots (between 1.5 and 2 mL) of solution were collected at pre-defined time intervals (1, 6 and 24 h), followed by filtration (0.22 µm nylon filters). The concentration of Ca^{2+} was determined through atomic absorption spectroscopy by flame atomization (AAS-FA) (details in section 2.6). Whenever the concentration of Ca^{2+} in solution became constant ($C_{Ca,e}$), corresponding to the solution-solid equilibrium, the experiment was stopped.

2.5.1. Effect of $C_{Ca,0}$ and m/V

The effect of $C_{Ca,0}$ in the sorption efficiency of GO and GO-Si(κ)CRG was evaluated for two metal concentrations: i) 30 mg L^{-1} (equivalent to 60 mg L^{-1} of $CaCO_3$) representing a soft water and ii) 120 mg L^{-1} (equivalent to 300 mg L^{-1} of $CaCO_3$) aiming to simulate hard water conditions. In these experiments, $m/V$of GO and GO-Si(κ)CRG was 1 g L^{-1}. Furthermore, the effect of m/V(0.50, 1.0, 2.0 and 5.0 g L^{-1}) of both nanomaterials in the efficiency of the sorption process was evaluated for a $C_{Ca,0}$ of 120 mg L^{-1}. In all studies, the experiments stopped after a contact time of 24 hours (solution-solid equilibrium). The samples were collected, followed by filtration and analysis by AAS-FA, as described in section 2.6.

2.5.2. Kinetics of GO-Si(κ)CRG–Ca^{2+} system

The adsorption kinetic of GO-Si(κ)CRG (material with the highest percentages of Ca^{2+} removal) was performed using the following experimental conditions: i) $C_{Ca,0}$=30 mg L^{-1} and m/V=1 g L^{-1} and ii) $C_{Ca,0}$=120 mg L^{-1} and m/V=5 g L^{-1}. After each period of contact (from 0 to 24 hours) the sample was collected, centrifuged and analysed by AAS-FA (procedure described in section 2.6), until equilibrium was reached.

2.5.3. Equilibrium studies of GO-Si(κ)CRG–Ca^{2+} system

The equilibrium data of GO-Si(κ)CRG were measured and the following experimental conditions were used: $C_{Ca,0}$=120 mg L^{-1} and varying m/V of GO-Si(κ)CRG from 0.50 to 15.0 g L^{-1}. The samples were collected after a period of contact of 24 h (to assure a situation of solution-solid equilibrium), followed by filtration and analysis by AAS-FA, as described in section 2.6.

2.5.4. Removal of other ions from bottled water

The concentration of copper (Cu), iron (Fe), magnesium (Mg), sodium (Na) and zinc (Zn) ions, occurring naturally in bottled water, was quantified for the sorption studies conducted with the following experimental conditions: i) $C_{Ca,0}$=30 mg/L and m/V of 1 g L^{-1} and ii) $C_{Ca,0}$=120 mg/L and m/V of 5 g L^{-1}. The samples were collected at 0 h and after a period of contact of 24 hours, filtered and the different elements were analysed, according with the procedure described in section 2.6.

Journal Pre-proof

2.6. Quantification of Ca^{2+} and other cations

The quantification of Ca^{2+} was performed by AAS-FA in a Perkin Elmer AAnalyst 100 spectrometer and using an air-acetylene flame. The concentration of Ca^{2+} was determined through a calibration curve of seven standards, with concentrations ranging from 0.0 to 6.0 mg L^{-1}. The standards were prepared in 0.25% KCl solution (ultrapure water) through dilution of the certified Ca^{2+} nitrate standard solution (1000 mg L^{-1}). In this concentration range, the detection limit of the method was 0.31 mg L^{-1}, with an acceptable relative standard deviation (RSD) <5%. The quantification of the other elements, i.e., copper (Cu), iron (Fe), sodium (Na) and zinc (Zn), was performed by ICP-OES Horiba Jobin Yvon model Activa M and equipped with a Burgener nebulizer. The calibration curves for these elements were obtained from dilution of certified standard solutions in a nitric acid solution (2% *v*/*v*) and with concentrations ranging from 0.4 to 40 mg L^{-1} for Mg and Na and from 4 to 400 μg L^{-1} Cu, Fe and Zn. The detection limit was 0.4 mg L^{-1} for Mg and Na and 4 μg L^{-1} for Cu, Fe and Zn, with an acceptable relative standard deviation <10%.

2.7. Evaluation of the softening capacity

The loading of Ca^{2+} in the GO and GO-Si(κ)CRG nanomaterials at a particular time *t* (q_t, mg g^{-1}) was determined by the material balance to the vessel between *t*=0 and *t*, according to equation (1):

$$q_{\mathrm{t}} = \frac{[C_{\mathrm{Ca},0} - C_{\mathrm{Ca}}(t)]V}{m_{\mathrm{NM}}} \qquad (1)$$

where $C_{\mathrm{Ca},0}$ (mg L^{-1}) is the initial concentration of Ca^{2+} in solution, $C_{\mathrm{Ca}}(t)$ (mg L^{-1}) is the concentration of Ca^{2+} at time *t*, *V* (L) is the volume of solution and m_{NM} (g) is the

mass of nanomaterial (GO or GO-Si(κ)CRG) used. The experimental results were also evaluated by the removal percentage at time *t* (R_t), defined by:

$$R_t = \frac{C_{Ca,0} - C_{Ca}(t)}{C_{ca,0}} \times 100 \quad (2)$$

At equilibrium, q_t and R_t are denoted as q_e and R_e, respectively.

2.8. Kinetic and equilibrium models

In the present study, the experimental data of Ca^{2+}/GO-Si(κ)CRG system was adjusted to theoretical kinetic (reaction and diffusion) models. The following reaction-based models were used: pseudo-first order ($P1^{st}O$), pseudo-second order ($P2^{nd}O$) and Elovich [30–32]. As for the diffusion-based models, Webber´s intraparticle diffusion and Boyd´s film diffusion were used to fit the experimental data [30,33,34]. The Ca^{2+} sorption capacity of GO-Si(κ)CRG was evaluated through isotherms studies, with the equilibrium data being modelled through the Langmuir and Freundlich equations [35–37]. The equations regarding the kinetic and equilibrium models are described in section S1 of supplementary material.

2.9. Error analysis of the data

Nonlinear regression analysis using GraphPad Prism 5 program (trial version), was used to determine the parameters for kinetic and equilibrium models, in which the least-squares and the Marquardt and Levenberg method are applied to adjust the variables. The fittings of the experimental data with the described models were confirmed calculating the sum of squares (*SS*), the correlation coefficient (R^2), and by interpretation of the Akaike´s Information Criterion (*AIC*) and the evidence ratio

(equations provided on section S2 of the supplementary material). Lower *AIC* values (on a scale from $-\infty$ to $+\infty$) suggest that the corresponding model adjusts better to the experimental data than the alternative models, and the evidence ratio is a numerical value that represents the number of times that the model with a lower *AIC* is more likely to be correct. [33].

The determination of parameters from the diffusion models and the critical analysis of the results was accomplished by piecewise linear regression methodology (PLR), using a Microsoft® Excel™ worksheet developed by Malash and El-Khaiary (2010) [33]. This methodology provides accurate information regarding the diffusion mechanisms involved, a better definition of the linear segments and correct determination of the diffusion coefficients.

2.10. Calcium speciation modeling

The speciation of calcium under the experimental conditions used was simulated by Visual MINTEQ, a software supported by the Swedish Research Council (VR) and by the Foundation for Strategic Environmental Research.

3. RESULTS AND DISCUSSION

3.1. Characterization of GO and GO-Si(κ)CRG

The envisaged sorption properties of the described hybrid softeners should stem from the effective surface modification of GO with the biopolymer κ-CRG via its alkoxide derivative (Si(κ)CRG). Therefore, the bare GO, the alkoxysilane derivative of carrageenan Si(κ)CRG and the prepared hybrid material GO-Si(κ)CRG were

chemically characterized by ATR-FTIR and Raman spectroscopy and elemental analysis. Also, the surface charge and the specific surface area (S_{BET}) were determined for GO and GO-Si(κ)CRG. The functionalization of GO with Si(κ)CRG was first confirmed by ATR-FTIR (Fig. 1A) and Raman (Fig. 1B) spectroscopies.

The ATR-FTIR spectrum for GO shows several characteristic vibrational bands [38]. The bands peaked at 1087 and 1222 cm^{-1} correspond to epoxy and alkoxy C–O stretching, respectively. The band at 1373 cm^{-1} is ascribed to the bending of tertiary C-OH groups [39]. The band at 1625 cm^{-1} is ascribed to aromatic C=C and O–H bending, the band peaked at 1702 cm^{-1} to C=O stretching, and the wide band centered at approximately 3230 cm^{-1} to the O–H stretching mode. Upon surface modification, several bands assigned to the siliceous κ-carrageenan are noticeable [40]. The characteristic vibrational bands of κ-carrageenan are observed at 1033-1058 cm^{-1} (C–O and C–OH stretching vibrations), 836 cm^{-1} (α(1-3)-D-galactose C–O–S stretching vibration) and 1222 cm^{-1} (O=S=O asymmetric stretching of sulfonate groups) [41]. The band at 1556 cm^{-1} may be indicative of N–H bending modes coupled to C–N stretching [42,43], while the peak at 1635 cm^{-1} may be ascribed to stretching vibration of hydrogen-bonded C=O in urea [44], much like what has been reported in nanomaterials using Si(κ)CRG as a functionalizing agent [28,40,45,46]. The ATR-FTIR spectrum of the alkoxide derivative of κ-carrageenan overlaps to some extent the GO bands. Still the disappearance of the band at ca. 1373 cm^{-1} might be ascribed to the reaction of C-OH groups of GO with the alkoxysilanes, via co-condensation reaction, thus corroborating surface modification.

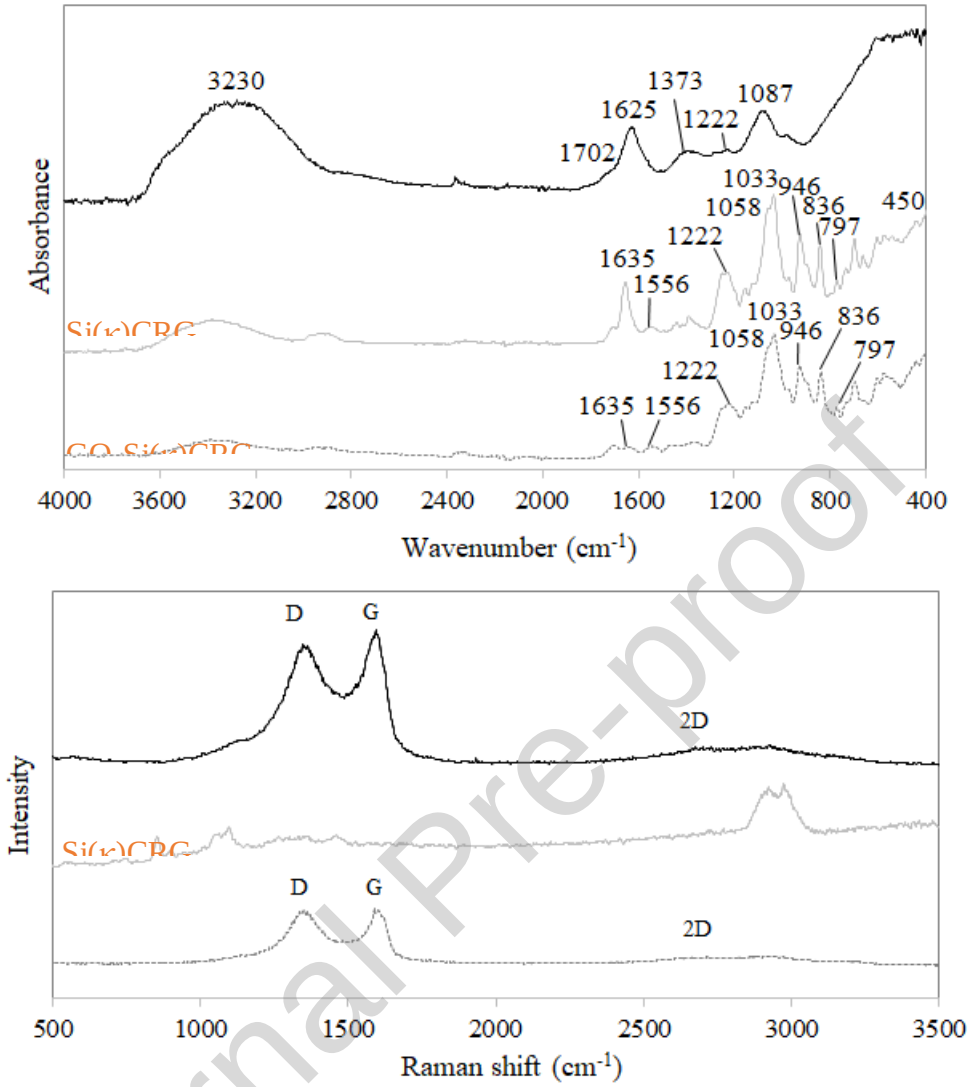

Figure 1. ATR-FTIR (A) and Raman (B) spectra for GO (—), Si(κ)CRG (—)and GO-Si(κ)CRG (¨).

Figure (1B) depicts the Raman spectra of the samples described above. For both GO and modified GO, the spectra show two bands at around 1350 and 1590 cm^{-1}. These are the D and G bands, respectively, and are typical of graphitic materials. The G band corresponds to the stretching of the C-C bond in ordered carbon structures having sp^2-hybridized C atoms. The D band is indicative of defects and disorder in the sp^2 structure, namely due to the presence of sp^3-hybridized C atoms bound to oxygen

Journal Pre-proof

functional groups [47,48]. The band intensity ratio I_D/I_G, indicative of carbon structure disorder, was 0.98 for both GO-based materials. This value is consistent with graphene-based materials, and also indicates no major changes in disorder during the surface modification process. The band centered at 2725 cm^{-1} in both materials corresponds to the 2D band. The 2D band is very sensitive to the defects and its broad peak indicates that the GO is dominated by the fully-disordered sp2 bonding network, being composed by stacking monolayers graphene sheets [49–52]. Furthermore, the intensity of this band is very low which is characteristic of GO. Pure graphene will display a stronger 2D band [48].

The Raman spectrum for the siliceous carrageenan shows less pronounced bands as compared to the other samples and also in comparison to the ATR-FTIR of the same sample, but a few characteristic bands can be assigned also for this case [53]. The band peaked at 854 cm^{-1} can be attributed to a C-O-SO_3^- group, the band at 1096 cm^{-1} is ascribed to a C-O bond in the 3,6-anhydrogalactose group, and finally, the peak at 1268 cm^{-1} is ascribed to the S=O bond. The band around 2900 cm^{-1} is ascribed to the -CH_2- stretching mode in ICPTES molecules present in the siliceous carrageenan [54]. While siliceous carrageenan dominated the ATR-FTIR spectra of the hybrid material, the reverse happens in the Raman spectra, where none of the aforementioned bands appear. This is in line with the sensitivity of Raman spectroscopy towards the characterization of extended carbon lattices having double carbon bonds, which are in great abundance in graphene-like materials [48].

Journal Pre-proof

Table 1 displays the elemental composition, specific surface area and porosity of the nanomaterials, as determined via elemental microanalysis and N_2 adsorption/ desorption isotherms.

Table 1. Physicochemical characterization of GO, Si(κ)CRG and GO-Si(κ)CRG: elemental composition (carbon, hydrogen, nitrogen and sulfur), specific surface area (S_{BET}) and total pore volume (V_p).

Material	Elemental composition (wt %)				S_{BET} (m^2 g^{-1})	V_p (cm^3 g^{-1})
	C	H	N	S		
GO	42.5±0.1	2.53±0.06	0.01±0.00	3.37±0.18	9.45	0.0100
Si(κ)CRG	32.4±0.1	4.83±0.06	2.59±0.04	3.87±0.45	---	---
GO-Si(κ)CRG	29.5±2.5	4.40±0.68	1.54±0.35	3.06±0.68	8.64	0.0065

The GO modification process causes a decrease in carbon content, that can be ascribed to the introduction of Si, and an increase in hydrogen and nitrogen, which is consistent with the introduction of siliceous carrageenan. Note that sulphur was also found in all the GO containing samples which is a consequence of the method used in the production of GO used as starting material [55] and, for the modified samples, is also due to the presence of sulfonate groups from carrageenan. Indeed, both spectroscopic and elemental microanalysis methods strongly suggest the successful incorporation of carrageenan into the GO structure. Table 1 shows that bare and modified GO present a low porosity, and this was reflected on the low values for the specific surface area. Typically, S_{BET} is strongly correlated with the adsorption efficiency, but in this

particular case, the identical values obtained for GO and GO-Si(κ)CRG, cannot infer on the adsorptive performance of both materials. This is likely more due to the presence of the biopolymer at the GO surfaces than to morphological changes occurring on the GO after surface modification. In fact, albeit showing some differences in thickness, both samples have shown a layered type morphology (non-porous materials) in the SEM analysis (Figure 2). Furthermore, the surface charge of the materials was assessed by electrophoretic mobility measurements at variable pH which is in line with this interpretation (Figure S1 of section S2 of the supplementary material). The zeta potential values obtained in these experiments showed for GO a negative surface charge between -23.5 ± 2.8 and -41.5 ± 2.7 mV, at a pH range from 2 to 11. In the case of the functionalized GO samples, the zeta potential values varied between -32.9 ± 2.5 and -38.6 ± 2.7 mV, which accounts for the observed colloidal stability. Since GO-Si(κ)CRG presents zeta potential values lower than −30 mV, according with Clogston and Patri (2011) [56], this hybrid material is considered strongly anionic, i.e. its surface charge is negative across the pH range studied. Additionally, more negative zeta potential values at acidic pH, observed in modified GO, are consistent with the presence of the sulfonated polysaccharide κ-carrageenan. The same was observed in other works that used κ-carrageenan as surface modifier [26]. The presence of sulfonate groups in GO-Si(κ)CRG is particularly advantageous for promoting electrostatic interactions with dissolved cationic species.

Journal Pre-proof

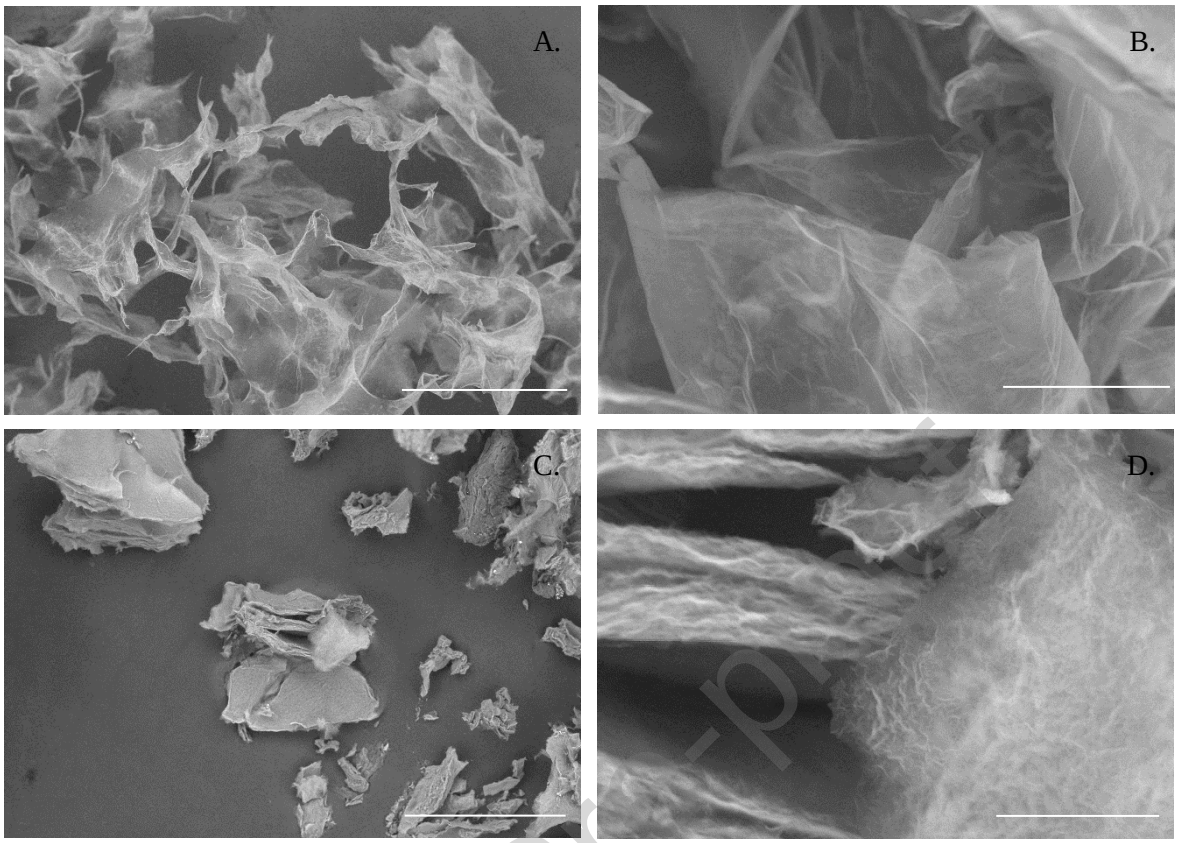

Figure 2. SEM images of the materials: GO (A and B) and GO-Si(κ)CRG (C and D). Magnifications used: 500× (A and C) and 5000× (B and D).

Effects of Ca^{2+} initial concentration and dose of softener on the removal efficiency

The efficiency of GO and GO-Si(κ)CRG in the removal of Ca^{2+} was investigated for two initial concentrations of Ca^{2+} (30 and 120 mg L^{-1}) and using a m/V of 1 g L^{-1} (Figure 3). At the pH values used to perform the adsorption experiments, the results highlighted that the modification of GO sheets with κ-CRG biopolymer improved the removal efficiency of Ca^{2+} (R_e, calculated by means of Eq. 2) from water, with values increasing from 23.8 to 77.7% ($C_{Ca,0}$=30 mg L^{-1}) and from 9.5 to 41.0% ($C_{Ca,0}$=120 mg L^{-1}). Regarding the values obtained for the sorption capacity at equilibrium (q_e, calculated using Eq. 1), an increment of *ca.* 3.3 and 3.9 times for $C_{Ca,0}$ of 30 and 120 mg L^{-1}, respectively, was observed after surface modification of GO.

These findings might be explained by an increase of the number of available active sites for Ca^{2+} binding as suggested above. The appearance of bands at 1222, 1556 and 1635 cm^{-1} in the FTIR spectrum of GO-Si(κ)CRG, corresponding respectively to vibrational modes of $–OSO_3^-$, N-H and C=O groups, support the existence of additional binding sites.

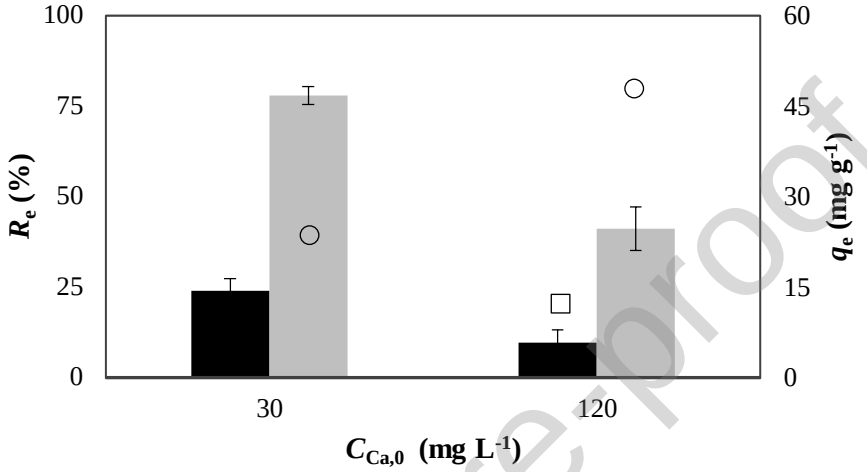

Figure 3. Values of R_e (%, columns) and q_e (mg g^{-1}, symbols) from spiked bottled water ($C_{Ca,0}$ of 30 and 120 mg L^{-1}) by means of GO (black column and □) and GO-Si(κ)CRG (grey column and ○). Experimental conditions: m/V= 1 g L^{-1} and pH *ca.* 7.

Furthermore, the sorption capacity (q_e) was dependent on the initial concentration of calcium ions ($C_{Ca,0}$). By increasing $C_{Ca,0}$ from 30 to 120 mg L^{-1}, the q_e increased from 23.5±0.5 mg g^{-1} to 47.8±4.3 mg g^{-1} for GO-Si(κ)CRG, and from 7.3±1.0 mg g^{-1} to 12.2±2.7 mg g^{-1} for GO. These results show that the initial Ca^{2+} concentration plays an important role in the adsorption process. Most likely, the initial concentration of calcium ions provides the necessary driving force to overcome the mass transfer resistance of Ca^{2+} from the aqueous phase to the solid phase. Thus, increasing $C_{Ca,0}$ shifts the sorption equilibrium towards adsorption, in accordance with the Le Chatelier's principle, and enhances the adsorption capacity. Regarding the removal

efficiency (R_e), it decreased from 77.7 to 41.0% for GO-Si(κ)CRG, and from 23.8 to 9.5% for the bare GO, when $C_{Ca,0}$ increased from 30 to 120 mg L^{-1}. Since the same m/V was used (1 g L^{-1}), these results can be explained because the available binding sites in both of GO and GO-Si(κ)CRG nanomaterials were not in enough number for complete Ca^{2+} removal for $C_{Ca,0}$ of 120 mg L^{-1}.

The effect of the amount (expressed by m/V) of GO and GO-Si(κ)CRG nanomaterials on the sorption process of Ca^{2+}, and starting with $C_{Ca,0}$ of 120 mg L^{-1}, was also evaluated in the present work. Figure 4 presents the values obtained for the removal of Ca^{2+} expressed in percentage (R_e, %) and by the amount of Ca^{2+} sorbed per gram of material at equilibrium (q_e, mg g^{-1}).

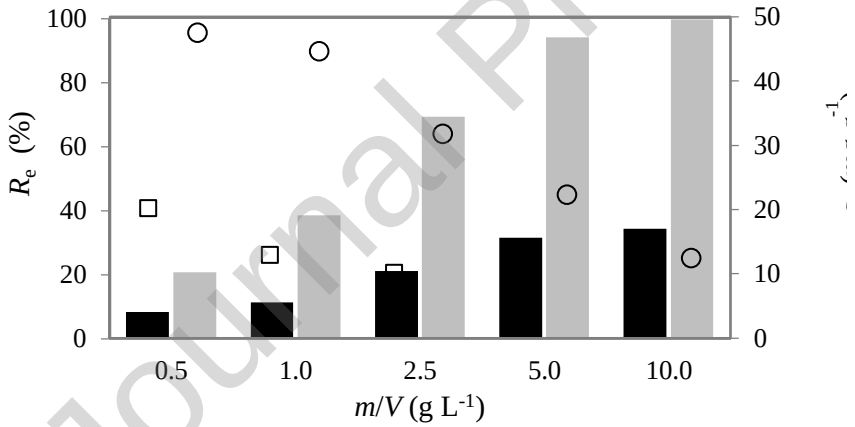

Figure 4. Values of R_e (%, columns) and q_e (mg g^{-1}, symbols) from spiked bottled water ($C_{Ca,0}$=120 mg L^{-1}) using different m/Vratios of the following materials: GO (black column and □) and GO-Si(κ)CRG (grey column and ○).

The results indicate that the removal efficiency of both GO and GO-Si(κ)CRG nanomaterials improved by increasing m/V ratio. By increasing the m/V from 0.25 to 5.0 g/L, an increase in R_e from 8.3 to 34.4% was attained for the non-modified GO, and

from 20.8 to 99.8% for the hybrid GO-Si(κ)CRG. This behavior can be explained by an increase of the available surface area, hence offering more sorption sites for Ca^{2+} binding. However, R_e does not change much for m/V≥5.0 g L^{-1} and tends towards a "*plateau*. In the case of GO material, this suggests that the removal efficiency does not depend on the amount of material used, i.e. on the available adsorption sites, indicating that a large number of active adsorption sites in GO nanomaterials remained free at higher m/V. As for the q_e values, an opposite tendency was observed, i.e. q_e decreased, increasing the m/V ratio. The lowest q_e values obtained ($m/V$of 10.0 g L^{-1}) were 4.3 and 12.4 mg g^{-1} for GO and GO-Si(κ)CRG, respectively, and the maximum q_e of 20.1 and 47.5 mg g^{-1} was reached for the lowest m/V (0.50 g L^{-1}). The obtained results indicate that the functionalization with the biopolymer κ-CRG considerably improves the efficiency of the bare GO, achieving identical percentages of Ca^{2+} removal (34 *vs* 38 % of GO and GO-Si(κ)CRG, respectively) with ten times less the amount m/V of material (10 g L^{-1} of GO and 1 g L^{-1} GO-Si(κ)CRG).

Additionally, the results on Figure 4 were converted into hardness units (by means of Eq. 3) and expressed as mg L^{-1} of $CaCO_3$ (Figure 5):

$$Hardness = \left(\frac{C_{Ca}}{M_{Ca}} + \frac{C_{Mg}}{M_{Mg}}\right) M_{CaCO3} \quad \text{Eq (3)}$$

where C_{Ca} and C_{Mg} is respectively the concentration of calcium and magnesium ions in solution, and M_{Ca} and M_{Mg} represents the atomic mass of calcium and magnesium, in the same order and M_{CaCO3} is the molar mass of $CaCO_3$. The C_{Mg} on the natural water used in the sorption experiments was very low (<0.47 mg L^{-1}), and because of this, the contribution from Mg^{2+} to hardness was negligible.

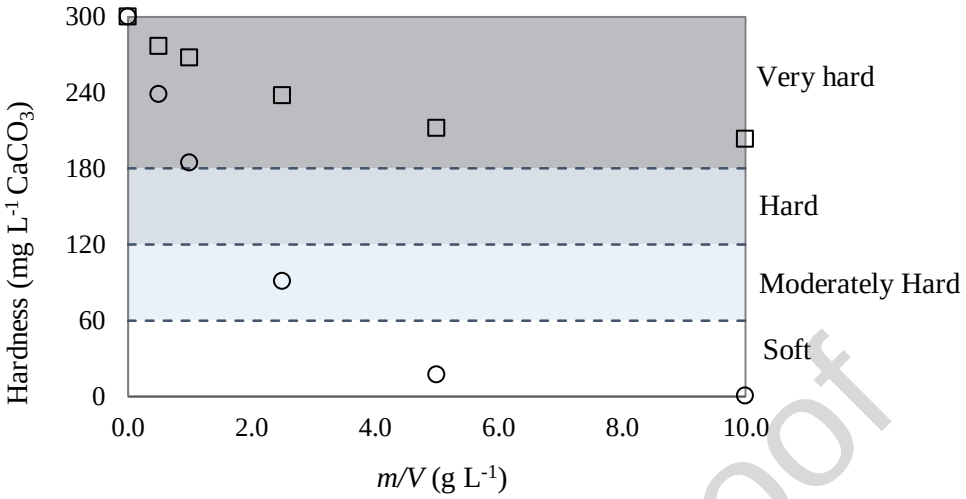

Figure 5. Effect of *m*/*V* ratio of GO (□) and GO-Si(κ)CRG (○) in reducing the levels of hardness (expressed in mg L^{-1} of $CaCO_3$) in very hard waters (300 mg L^{-1} of $CaCO_3$ prepared in bottled water).

In the case of GO and within all the m/V range studied (0.5 and 10 g L^{-1}), the material was not effective and after water treatment the levels of $CaCO_3$ found were still characteristic of a very hard water (>180 mg L^{-1} of $CaCO_3$). As for GO-Si(κ)CRG, its efficacy was highly dependent on m/V used. When a m/V ratio of 0.5 g L^{-1} of GO-Si(κ)CRG was used the sorption process was not suitable to reduce the levels of hardness of spiked bottled waters (180 mg L^{-1} of $CaCO_3$). Increasing the m/V ratio of GO-Si(κ)CRG to 1.0 and 2.5 g L^{-1}, at the end of the sorption procedure the water was classified as hard (between 120 and 180 mg L^{-1} of $CaCO_3$) and moderately hard (between 60 and 120 mg L^{-1} of $CaCO_3$), respectively. Finally, for a m/V ratio of 5.0 and 10 g L^{-1} of GO-Si(κ)CRG the procedure was extremely efficient, being able to convert a very hard water into a soft water (< 60 mg L^{-1} of $CaCO_3$). Due to the performance

exhibited by GO-Si(κ)CRG nanomaterial in hard water treatment, this was the material selected for the following studies.

3.3. Kinetic studies

The kinetic curves for the sorption of Ca^{2+} onto GO-Si(κ)CRG were established in order to evaluate the time required to reach the equilibrium between the liquid and the solid phases. Figure 6 shows the variation of the normalized concentration of Ca^{2+} from bottled water ($C_{Ca,t}/C_{Ca,0}$) with time (t), for the following experimental conditions: i) $C_{a,0}$ of 30 mg L^{-1} and m/V of 1 g L^{-1} and ii) $C_{a,0}$ of 120 mg L^{-1} and m/V of 5 g L^{-1}.

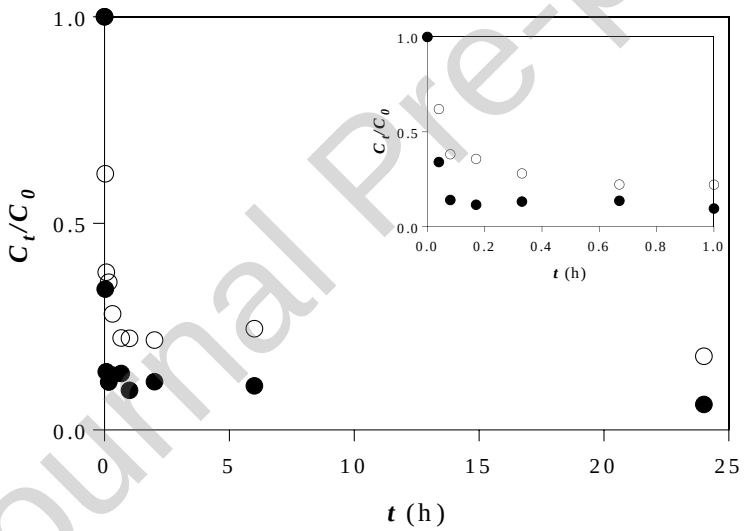

Figure 6. Variation of C_t/C_0 with t (h) for Ca^{2+}/GO-Si(κ)CRG system under different experimental conditions: $C_{Ca,0}$=30 mg L^{-1} and m/V=1.0 g L^{-1} (○) and $C_{Ca,0}$=120 mg L^{-1} and m/V=5.0 g L^{-1} (●), for a total contact time of 24h (Inset: variation of C_t/C_0 in the first hour).

The kinetic profiles are characterized by an abrupt decrease on Ca^{2+} levels up to 2.5 to 5 minutes contact time, thus indicating fast calcium uptake by the GO-Si(κ)CRG material. The equilibrium is attained after a period of contact of 20 minutes for $C_{Ca,0}$ of

30 mg L^{-1} (*m*/*V* of 1.0 g L^{-1}) and 10 minutes for 120 mg L^{-1} (*m*/*V* of 5.0 g L^{-1}), with percentages of Ca^{2+} removal of 77.7±2.5% and 89.3±1.1%, respectively. Additionally, control experiments (without the adsorbent material) were run in parallel (data not presented) and the deviations found were less than 5%.

The adsorption kinetic data obtained for the Ca^{2+}GO-Si(*k*)CRG system were fitted with both surface reaction- and diffusion-based models, for both experimental conditions, and the results are presented in Table 2.

Table 2. Experimental data at equilibrium ($C_{Ca,e}$ R_e, q_e) and modelling results for the Ca^{2+}/GO-Si(κ)CRG system by using reaction-based and diffusion-based kinetic models.

		$C_{Ca,0}$= 30 mg L^{-1} dose= 1 g L^{-1}	**$C_{Ca,0}$= 120 mg L^{-1} dose= 5 g L^{-1}**
Experimental data	$C_{Ca,e}$ (mg L^{-1})	6.98±0.80	12.5±1.2
	R_e (%)	77.7±2.5	89.3±1.1
	q_e^{exp} (mg g^{-1})	23.5±0.5	21.0±0.4
Reaction models			
P1stO	q_e^{fit} (mg g^{-1})	23.2±0.3	20.9±0.1
	k_1 (h^{-1})	20.8±1.7	32.2±1.3
	R^2	0.988	0.998
	SS	6.13	0.760
	AIC	0.822	-20.1

	q_e^{fit} (mg g^{-1})	23.8±0.4	21.4
	k_2 (g mg^{-1} h^{-1})	1.49±0.26	3.48
P2ndO	R^2	0.981	0.995
	SS	10.1	2.15
	AIC	5.77	-9.64
	β (g mg^{-1})	0.766±0.22	1.49±0.51
	α (mg g^{-1} h^{-1})	1.69×10^{7}	9.42×10^{12}
Elovich	R^2	0.914	0.963
	SS	45.9	14.5
	AIC	20.9	9.40
	Diffusion models		
Boyd´s plot	Interval of intercept	[0.269; 0.289]	[0.371; 0.441]
	R^2	0.998	0.985
Webber plot	1st Stage: k_{id} (mg g^{-1} $h^{-1/2}$)	95.2	62.8
	Intercept (mg g^{-1})	-6.94	1.44
	R^2	1.00	1.00
	2nd Stage: k_{id} (mg g^{-1} $h^{-1/2}$)	5.78 ± 0.18	5.03 ± 1.71

Journal Pre-proof

R^2	0.999	0.896
3rd Stage: k_{id} (mg g^{-1} $h^{-1/2}$)	0.114 ± 0.152	0.091 ± 0.095
R^2	0.220	0.234

i) Reaction-based models

The experimental kinetic data was fitted with the non-linear forms of pseudo-first order (P1stO, Eq. S1 of supplementary material), pseudo-second order (P2ndO, Eq. S2 of supplementary material) and Elovich (Eq. S3 of supplementary material) models (Figure 7) and the adjusted parameter´s values are listed in Table 2. These models assume the rate of surface reaction as the rate-limiting step.

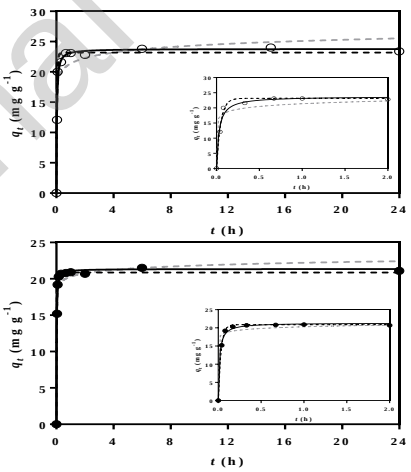

Figure 7. Kinetic modelling of the experimental data obtained for Ca^{2+}/GO-Si(κ)CRG system (○ and ●) system using P1stO (- -), P2ndO (—), and Elovich (- -) models. Experimental conditions: $C_{Ca,0}$=30 mg L^{-1}, m/V=1.0 g L^{-1} (○) and $C_{Ca,0}$=120 mg L^{-1}, m/V=5.0 g L^{-1} (●).

Under the experimental conditions used, a good agreement was observed between the experimental kinetic data and both P1stO and P2ndO models, with R^2 values ranging between 0.981 and 0.998. The equilibrium concentration calculated (q_e^{fit}) for each of the P1stO and P2ndO models is close to the experimental values (q_e^{exp}) of 23.5 mg g^{-1} (Table 2), with relative errors below 2%. A closer look at Akaike´s Information Criterion (*AIC*) (details provided in section S2 of the supplementary material), revealed that the lowest values (for both experimental conditions) are achieved with P1stO model (Table 2), indicating that this model is better adjusted to the experimental data. Additionally, the evidence ratio parameter was calculated and according to the obtained values, the P1stO model is 12 ($C_{Ca,0}$=30 mg L^{-1} and m/V=1.0 g L^{-1}) and 183 ($C_{Ca,0}$=120 mg L^{-1}, and m/V=5.0 g L^{-1}) times more likely to be correct than the P-2ndO model, and 2.3×10^4 ($C_{Ca,0}$=30 mg L^{-1} and m/V=1.0 g L^{-1}) and 2.5×10^6 ($C_{Ca,0}$=120 mg L^{-1}, and m/V=5.0 g L^{-1}) times than the Elovich model.

ii) Diffusion-based models

To ascertain information regarding the mechanism and rate-controlling steps affecting the sorption process of Ca^{2+} onto GO-Si(κ)CRG, the Boyd's film diffusion (Eq. S5 and S6, supplementary material) and Webber's pore diffusion (Eq. S4, supplementary material) models were applied. Piecewise linear regression (PLR) was applied to the experimental data for both Ca^{2+} initial concentrations (and different GO-Si(κ)CRG dose) and the corresponding data is presented in Table 2.

From the Boyd´s plot (Bt *vs* t, Figure S2 supplementary material) a linear segment (R^2>0.985) is obtained in the beginning of the sorption process (t ≤ 20 minutes). The values obtained for the intercept (Table 2) are significantly different from

zero (with 95% confidence limits), suggesting that film diffusion is the rate controlling mechanism in the initial stage (*ca.* 20 minutes) of the sorption process of adsorption [5733 58].

The Webber's plots (q_t vs $t^{1/2}$) obtained (Figure 8) indicate the existence of three operational stages.

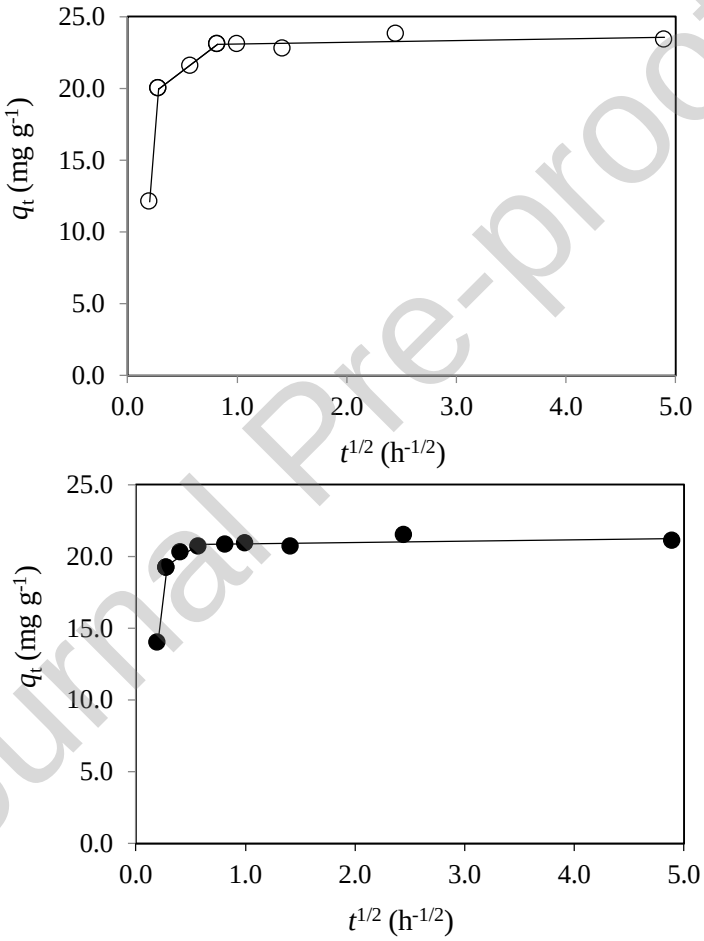

Figure 8. Kinetic modeling of the experimental data of the adsorption process of Ca^{2+} onto GO-Si(κ)CRG by using the Webber´s intraparticle diffusion model, for the following experimental conditions: $C_{Ca,0}$=30 mg L^{-1} e m/V=1.0 g L^{-1} (○) e $C_{Ca,0}$=120 mg L^{-1} e m/V=5.0 g L^{-1} (●).

The first stage corresponds to the steep-sloped portion of q_t *vs* $t^{1/2}$ plot and includes the initial sorption period (5 minutes), which involves external diffusion and binding of Ca^{2+} ions to the active sites distributed on the outer surface of the GO-Si(κ)CRG particles. The second stage, ranging between 5 minutes and 40 or 60 minutes (depending on the experimental conditions used), includes a sloped linear portion less marked and involves the intra-particle diffusion and binding of Ca^{2+} by the active sites distributed on macropores, mesopores and micropores of GO-Si(κ)CRG material. The third and final stage corresponds to equilibrium, which is achieved for t> 40 ($C_{Ca,0}$=120 mg L^{-1}, and m/V=5.0 g L^{-1}) and 60 ($C_{Ca,0}$=30 mg L^{-1} and m/V=1.0 g L^{-1}) minutes. The results also indicate that under the mentioned experimental conditions, in which $C_{Ca,0}$ and m/V were simultaneously changed, the values obtained for the internal diffusion rate constant (K_{id}) in all the three stages, were always higher for $C_{Ca,0}$ of 30 mg L^{-1} and m/V of 1.0 g L^{-1}. This suggests that under these particular conditions, in opposition to the results obtained by Ofomaja (2010) [59], the expected increment in the concentration gradient for higher $C_{Ca,0,}$ causing a faster diffusion, was not observed.

The values obtained for the intercept of the first linear segment on Webber´s plot were different from zero (Table 2) suggesting that pore diffusion does not control the sorption process of Ca^{2+} by GO-Si(κ)CRG material. These results are in agreement with the results from Boyd's plots, i.e. that the sorption process is controlled by film diffusion in the initial period of sorption [33,57,58]. This means that this step contributes dominantly to the total resistance in the beginning of the adsorption process in GO-Si(κ)CRG, and the contribution from pore diffusion and surface reaction is irrelevant. According with Tran et al. (2017), this behavior is expected for non-porous adsorbents [60], such as GO-Si(κ)CRG. Besides that, the multi-linear nature observed in Boyd's and

Webber's plots is indicative that the overall sorption rate process is controlled by both film and pore diffusion [33].

At this point, it should be mentioned that besides diffusion models, kinetic results were also well described by pseudo-first-order model, and that pseudo-second-order model was found less adequate. These findings agree with the literature because an assumption of the pseudo-second order model is that the adsorption process is not limited by diffusion [61]. Other authors also reported that the pseudo-second order model is not adequate to describe diffusion-controlled sorption processes [62].

Sorption equilibrium models

The isotherm describes the equilibrium distribution of the species to be removed between the liquid and solid phases, and it represents a key tool in any adsorption system. The isotherms of Ca^{2+}–GO-Si(κ)CRG system in spiked bottled water were assessed by collecting the data from the equilibrium experiments and fitting with the non-linear models of Langmuir (L) and Freundlich (F) (Eq. S7 and S8 of supplementary material, respectively) isotherms (Figure 9).

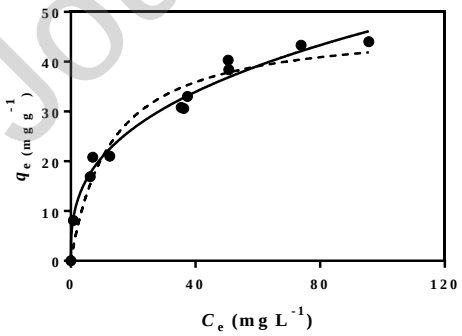

Figure 9. Experimental equilibrium data for Ca^{2+}–GO-Si(κ)CRG system at 21±1ºC, together with modeling results: Langmuir (---) and Freundlich (—) isotherms.

The analysis of these plots showed that the Freundlich model provides a better fitting across the concentration range studied. This can be confirmed by the higher R^2 and also by the lowest sum of squares (S*S*) value ($SS_{Freundlich}$=36.7 vs $SS_{Langmuir}$=113) obtained by fitting the experimental results with Freundlich model (Table 3).

Table 3. Isotherm fitting parameters for Ca^{2+}–GO-Si(κ)CRG system.

Langmuir			**Freundlich**		
q_{mL} (mg g^{-1})	a_L (L mg^{-1})	R^2	K_F ($mg^{1-1/n} L^{1/n} g^{-1}$)	*n'*	R^2
47.6±3.2	(7.70±1.93)×10^{-2}	0.948	9.24±0.87	2.84±0.20	0.983

The *AIC* values ($AIC_{Freundlich}$=18.8 < $AIC_{Langmuir}$ =32.2) and the evidence ratio indicate that Freundlich model is 855 times more likely to be correct than the Langmuir model. In addition, these results suggest that multilayer adsorption may occur and the value of 0.35 obtained for the sorption heterogeneity 1/*n*' is indicative of a favorable sorption process of Ca^{2+} and the heterogeneity of GO-Si(κ)CRG surface sites. Also, the L-type convex shape of the isotherm suggests the favorable sorption of Ca^{2+} within the interval of C_e used. To get further insight about the nature of the interaction between Ca^{2+} and the GO-Si(κ)CRG sorbent, the standard free energy change (ΔG°) was estimated from the isotherm experimental data obtained at 21 ± 2.0 °C (see Supplementary Material) [63]. The calculated ΔG° was -19.67 kJ mol^{-1}, indicating spontaneous adsorption of Ca^{2+}on the surface of the sorbent.

The Langmuir isotherm provided a maximum sorption capacity at monolayer coverage, q_{mL} of 47.6±3.2 mg g^{-1}. The determination of q_{mL} is also useful to evaluate the performance of distinct adsorbent materials, since it allows the quantitative comparison of the adsorption capacity. Table 4 presents the values found in the literature for the maximum adsorption capacity obtained (q_{mL}), the time needed to reach equilibrium (t_e) and the experimental conditions used for the removal of Ca^{2+} using different adsorbent materials.

Table 4. Values obtained for the maximum adsorption capacity (q_{mL}), time to reach equilibrium (t_e) and the experimental conditions (pH, m/V and $C_{Ca,0}$) for the removal of Ca^{2+} using different materials.

Material	m/V (g/L)	$C_{Ca,o}$ (mg L^{-1})	pH	t_e	q_{mL} (mg g^{-1})	Reference
• (a) Silica nanoparticles • (b) Fungus *F. verticillioides* immobilized on Silica	1.5	[40-2.0×10^3]	7	$C_{Ca,0}$ =400 mg L^{-1} • 20 min (all materials)	• (a) 68.49 • (b) 92.59	[11]
• (a) Natural pumice stones • (b) Alkaline modified pumice stones	6	[25-150]	6	$C_{Ca,0}$ =150 mg L^{-1} • (a) >240 min • (b) 150 min	• (a) 62.34 • (b) 52.27	[12]
•Bentonite clay modified with SDBS	1.5	120	---	C_{CaCO3}=120 mg L^{-1} • 75 min	• 14.63	[13]

• Oxidized carbon nanotubes	2.0	[100-1200]	---	C_{CaCO3}=100 mg L^{-1} • 30 min	• 79.64	[10]
• (a) Mercerized cellulose • (b) Sugarcane bagasse chemically modified with EDTAD	1	[30-75]	5.5	$C_{Ca,0}$ =85 mg L^{-1} • 10 min	• (a) 15.6 • (b) 46.1	[9]
Anionic-cellulose nanofibers	1.3	[25-400]	7.0	$C_{Ca,0}$ =25 mg L^{-1} • 60 min	57.66	[64]
Sodium-modified vermiculite	20	[500-2000]	10	$C_{Ca,0}$ =25 mg L^{-1} • 90 min	45.43	[65]
• GO-Si(κ)CRG	0.5-15	120	6.5	$C_{Ca,0}$ =120 mg L^{-1} • 10 min	• 47.6	Present study

SDBS: Sodium dodecyl benzene sulfonate, EDTAD: Ethylenediamine tetraacetic acid dianhydride

The maximum sorption capacity of GO-Si(κ)CRG for Ca^{2+} was identical to the values found in the literature for natural and modified pumice stones [12] and sodium-modified vermiculite [65] and other carbon-based materials, namely sugarcane bagasse modified with EDTAD [9] and anionic-cellulose nanofibers [64]. Higher q_m values were exhibited by bare and modified silica nanoparticles [11] and also by oxidized carbon nanotubes [10], which might be attributed to the high specific surface area of both silica (S_{BET}=140–180 m^2 g^{-1}) [11] and carbon nanotube based materials [10]. As for chemically modified bentonite [13] and mercerized cellulose [9], the values obtained for q_m were ca.

three times lower than that of GO-Si(κ)CRG. These results show the potential of GO-Si(κ)CRG material for hard water softening.

3.4. Removal of other ions naturally occurring in bottled water

The removal of other ions, some of them contributing for water hardening, was evaluated in the present work. Table 5 presents the concentration of Ca^{2+} and Mg^{2+} (hard ions) and corresponding hardness, and the concentration of Na^{+} in the following samples: bottled water (BW), spiked bottled water with variable Ca^{2+} concentration prior (control) and after treatment with GO-Si(κ)CRG. These essays were conducted using the following experimental conditions: 1) $C_{Ca,0}$=30 mg L^{-1} and m/V of 1 g L^{-1} and 2) $C_{Ca,0}$=120 mg L^{-1} and m/V of 5 g L^{-1}.

Table 5. Hardness and concentration of major (Ca, Mg and Na) and minor cations (Cu, Zn and Fe) obtained in bottled water (BW) and bottled water spiked with Ca^{2+} prior (control) and after treatment with GO-Si(κ)CRG. Experimental conditions used: (1) $C_{Ca,0}$=33 mg L^{-1} and m/V of 1 g L^{-1} and (2) $C_{Ca,0}$=113 mg/L and m/V of 5 g L^{-1}.

	Ca	**Mg**	**Hardness**	**Na**	**Cu**	**Zn**	**Fe**
	mg/L	**mg/L**	**mg/L**	**mg/L**	**µg/L**	**µg/L**	**µg/L**
BW	3.40	0.43	10.3	4.60	< 4	< 10	< 10
Control 1	32.3	0.43	82.6	5.30	< 4	< 10	< 10
GO-Si(κ)CRG 1	4.52	0.20	12.1	6.50	< 4	< 10	< 10
Control 2	112.8	0.43	284	6.40	< 4	< 10	< 10

GO-Si(κ)CRG 2	7.03	0.16	18.2	13.0	< 4	< 10	< 10

The results show that the levels of Mg and Na found in the bottled water, before (BW) and after spiking with Ca^{2+} solution (Control 1 and 2), were low and the values for these cations ranged between 0.43 and 6.4 mg L^{-1}. The levels found for Cu, Zn and Fe minor elements in all analysed samples were below the limit of quantification of ICP-OES. After treatment with GO-Si(κ)CRG, the concentration of Ca^{2+} decreased to values lower than 7 mg L^{-1} and the removal efficiencies were about 86 and 97%, starting with $C_{Ca,0}$ of 33 and 113 mg L^{-1}, respectively. The values obtained were slightly higher than those indicated in section 3.2, but still, the percentages of removal were quite identical. In the case of Mg and despite the small concentration found in both controls, the concentration decreased in the presence of GO-Si(κ)CRG and the removal efficiency was estimated as 53 and 63%, for $C_{Ca,0}$ of 33 and 113 mg L^{-1}. The speciation of Ca and Mg under the experimental conditions used was simulated by Visual MINTEQ and the results showed that 99% of the dominant species in solution are Ca^{2+} and Mg^{2+}, for both cations, and less than 1% are presented as $CaCl^{+}$ and $MgCl^{+}$. Therefore, and due to the presence of anionic sulfonate groups at GO-Si(κ)CRG surface, the electrostatic attraction is likely to be the main sorbate–sorbent mechanism involved. The FTIR-ATR analysis of GO-Si(κ)CRG sorbent after being in contact with a Ca^{2+} aqueous solution shows a shift on the O=S=O asymmetric stretching band of sulfonate groups of κ-carrageenan to lower wavenumbers, from 1222 cm^{-1} to 1193 cm^{-1} (Figure S3-supplementary material), which suggests that the sulfonate groups interact

with Ca^{2+} cations. Indeed, a similar effect has been reported for FTIR spectroscopic analysis of the interaction of carrageenan with other cations, namely Fe^{2+} and Fe^{3+}[66]. Besides, Ca^{2+} and Mg^{2+} can establish stable bonds with oxygen-containing ligands (e.g. OH− and -C=O) [67]. Furthermore, the increment found in the concentration of Na after the sorption process with GO-Si(κ)CRG material, suggests that an ion exchange mechanism might also contribute to the sorption process of Ca and Mg ions by GO-Si(κ)CRG.

The simultaneous removal of Ca^{2+} and Mg^{2+} (the two main cations responsible for causing hardness) from bottled water by GO-Si(κ)CRG was also evaluated and the results were compared with that of Ca^{2+} single spiked samples (Figure 10). The experiments were performed in binary solutions containing Ca^{2+} and Mg^{2+} with an initial concentration of 30 mg L^{-1} and 12 mg L^{-1}, respectively (corresponding to a total hardness of 125 mg L^{-1} of $CaCO_3$). According with the WHO the levels of Mg^{2+} typically found in natural waters are lower than that of Ca^{2+} [68], and for that reason the sorption experiments were carried out using a Mg^{2+} concentration ca. 2.5 times lower than that of Ca^{2+}.

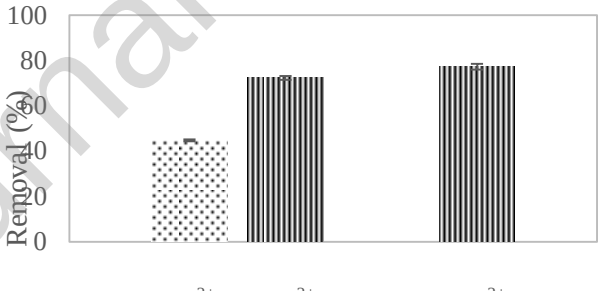

Figure 10. Removal (R_e) of Ca^{2+} from single spiked bottled water ($C_{Ca,0}$ of 30 mg L^{-1}) and Ca^{2+} and Mg^{2+} from binary spiked bottled water ($C_{Ca,0}$ of 30 mg L^{-1} and $C_{Mg,0}$ of 12 mg L^{-1}) by GO-Si(κ)CRG. Other experimental conditions: m/V= 1 g L^{-1} and pH *ca.* 7.

The results showed that under the experimental conditions used, the removal of Ca^{2+} was not significantly affected by the presence of Mg^{2+}, and the percentage of 72.4±0.9 % of Ca^{2+} removed in the mixed solution was identical to that of 77.7±0.9 %

in single spiked solution. Besides that, in both single and binary solutions the equilibrium was attained after a period of contact of 40 to 60 minutes (data not shown).

4. CONCLUSIONS

In this research, we have demonstrated for the first time the functionalization of GO through the grafting of the polysaccharide *κ*-carrageenan aiming at developing more environmentally friendly water softeners. It was found that the adsorptive capacity of the hybrid GO-Si(κ)CRG to remove Ca^{2+} and other dissolved ions from bottled water improved, as compared to non-functionalized GO samples, likely due to electrostatic interactions between metal cations and the negatively charged polymer. As expected, the efficiency of GO-Si(κ)CRG in the softening process was shown to be dependent on the experimental conditions, with higher Ca levels requiring the use of higher amount of sorbent, for the same volume of water. Nevertheless, the hybrid GO-Si(κ)CRG was successfully applied to convert very hard water (300 mg L^{-1} of $CaCO_3$) in soft water, i.e. below 60 mg L^{-1} of $CaCO_3$, whose performance was not altered by the presence of other ions typically found in natural bottled waters.

Finally, we surmise that the surface modification described here may have implications for the development of a new class of water softeners based on GO materials. The wide range of biopolymers extracted from renewal sources can be further explored in GO functionalization, in order to achieve environmental friendly adsorbents for water softening technology. The authors envision finding environmentally friendly and efficient regeneration processes that will allow the reuse of this material and their cost-effective implementation in real scale applications. The treatment of aqueous suspensions of the sorbents, at a mild temperature but that allows the unfolding of the

GO-grafted biopolymer chains with consequent release of the calcium ions is an unexplored approach that avoids exchange processes using concentrated brine. Therefore studies are in progress that involve monitoring the regeneration of GO-Si(k)CRG, and assess its sorption capability after multiple cycles of reuse and regeneration.

5. ACKNOWLEDGEMENTS

This work was developed within the scope of the project CICECO-Aveiro Institute of Materials, FCT Ref. UIDB/50011/2020 & UIDP/50011/2020 and TEMA, UID/EMS/00481/2013-FCT, financed by national funds through the FCT/MCTES and when appropriate co-financed by FEDER under the PT2020 Partnership Agreement. This work was developed in the scope of the "Smart Green Homes" Project [POCI-01-0247-FEDER-007678], a co-promotion between Bosch Termotecnologia S.A. and the University of Aveiro, funded by Portugal 2020 under the Competitiveness and Internationalization Operational Program, and by the European Regional Development Fund. Acknowledge is also made to H_2O Value project: CENTRO-01-0145-FEDER-030513 e PTDC/NAN-MAT/30513/2017. The costs resulting from the FCT hiring is funded by national funds (OE), through FCT, I. P. in the scope of the framework contract foreseen in the numbers 4, 5 and 6 of the article 23, of the Decree-Law 57/2016, of August 29. A.L. Daniel-da-Silva acknowledges FCT IF/00405/2014 grant.

6. REFERENCES

1 K. S. Brastad and Z. He, *Desalination*, 2013, **309**, 32–37.

2 J. Choi, P. Dorji, H. K. Shon and S. Hong, *Desalination*, 2019, **449**, 118–130.

3 S. Akram and Fazal-ur-Rehman, *J. Chem. Appl.*, 2018, **4**, 1–4.

4 WHO, *Hardness in Drinking-water (WHO/HSE/WSH/10.01/10/Rev/1)*, 2011.

5 A. K. Sengupta, *Environ. Sci. Technol.*, 2006, **40**, 370–376.

6 G. Cetin, *ISRN Anal. Chem.*, 2014, **2014**, 1–7.

7 U. Pratomo, A. Anggraeni, R. A. Lubis, A. Pramudya and I. N. Farida, *Procedia Chem.*, 2015, **16**, 400–406.

8 J. Li, S. Koner, M. German and A. K. Sengupta, *Environ. Sci. Technol.*, 2016, **50**, 11943–11950.

9 O. Karnitz, L. V. A. Gurgel and L. F. Gil, *Carbohydr. Polym.*, 2010, **79**, 184–191.

10 M. A. Tofighy and T. Mohammadi, *Desalination*, 2011, **268**, 208–213.

11 M. E. Mahmoud, A. A. Yakout, H. Abdel-Aal and M. M. Osman, *Bioresour. Technol.*, 2013, **134**, 324–330.

12 M. N. Sepehr, M. Zarrabi, H. Kazemian, A. Amrane, K. Yaghmaiand and H. R. Ghaffari, *Appl. Surf. Sci.*, 2013, **274**, 295–305.

13 N. nadia A. Kadir, M. Shahadat and S. Ismail, *Appl. Clay Sci.*, 2017, **137**, 168–175.

14 A. Bessa, G. Gonçalves, B. Henriques, E. M. Domingues, E. Pereira and P. A. A. P. Marques, *Nanomaterials*, 2020, **10**, 1–16.

15 L. Sun, *Chinese J. Chem. Eng.*, 2019, **27**, 2251–2260.

16 I. L. Laure, S. V Tkachev, E. Y. Buslaeva, E. V Fatushina and S. P. Gubin, 2013, **39**, 487–492.

17 L. Jiajie, H. Yi, Z. Fan, Z. Yi, L. I. Ning and C. Yongsheng, *Sci. China Technol. Sci.*, 2014, **57**, 284–287.

18 B. Henriques, G. Gonçalves, N. Emami, E. Pereira, M. Vila and P. A. A. P. Marques, *J. Hazard. Mater.*, 2016, **301**, 453–461.

19 C. Zhang, W. Wang, A. Duan, G. Zeng, D. Huang, C. Lai, X. Tan, M. Cheng, R. Wang, C. Zhou, W. Xiong and Y. Yang, *Chemosphere*, 2019, **222**, 184–194.

Journal Pre-proof

20 M. Yang, X. Liu, Y. Qi, W. Sun and Y. Men, *J. Colloid Interface Sci.*, 2017, **506**, 669–677.

21 B. H. Henriques, G. Gonçalves, N. Emamie, E. Pereira, M. Vila and P. A. A. P. Marques, *J. Hazard. Mater.*, 2016, **301**, 453–461.

22 G. R. Mahdavinia, H. Aghaie, H. Sheykhloie, M. T. Vardini and H. Etemadi, *Carbohydr. Polym.*, 2013, **98**, 358–365.

23 O. Duman, S. Tunç, T. G. Polat and B. K. I. Bozoğlan, *Carbohydr. Polym.*, 2016, **147**, 79–88.

24 M. El Hefnawy, K. A. Ali and M. M. D. Allah, *Chem. Process Eng. Res.*, 2018, **58**, 6–16.

25 A. L. Daniel-da-Silva, A. M. Salgueiro, B. Creaney, R. Oliveira-Silva, N. J. O. Silva and T. Trindade, *J. Nanoparticle Res.*, 2015, **17**, 1–15.

26 T. Fernandes, S. F. Soares, T. Trindade and A. L. Daniel-Da-silva, *Nanomaterials*, , DOI:10.3390/nano7030068.

27 S. F. Soares, T. R. Simões, T. Trindade and A. L. Daniel-da-silva, *Water. Air. Soil Pollut.*, , DOI:10.1007/s11270-017-3281-0.

28 S. F. Soares, T. Trindade and A. L. Daniel-da-silva, *Eur. J. Inorg. Chem.*, 2015, 4588–4594.

29 A. M. Dimiev, L. B. Alemany and J. M. Tour, *ACS Nano*, 2013, **7**, 576–588.

30 Y. S. Ho, J. C. Y. Ng and G. McKay, *Sep. Purif. Methods*, 2000, **29**, 189–232.

31 Y. S. Ho, *J. Hazard. Mater.*, 2006, **136**, 681–689.

32 G. Crini, E. Lichtfouse, L. Wilson, N. Morin-crini, G. Crini, E. Lichtfouse, L. Wilson, N. M. Adsorption-oriented, G. Crini, E. Lichtfouse, L. D. Wilson and N. Morin-crini, *Adsorption-oriented processes using conventional and non-conventional adsorbents for wastewater treatment. Green Adsorbents for Pollutant Removal*, Springer Nature, 2018.

33 G. F. Malash and M. I. El-Khaiary, *Chem. Eng. J.*, 2010, **163**, 256–263.

Journal Pre-proof

34 M. I. El-Khaiary and G. F. Malash, *Hydrometallurgy*, 2011, **105**, 314–320.

35 J. Wang and C. Chen, *Biotechnol. Adv.*, 2009, **27**, 195–226.

36 Y. S. Ho, J. F. Porter and G. Mckay, *Water. Air. Soil Pollut.*, 2002, **141**, 1–33.

37 E. I. El-Shafey, *J. Hazard. Mater.*, 2010, **175**, 319–327.

38 V. H. Pham, T. V. Cuong, S. H. Hur, E. Oh, E. J. Kim, E. W. Shin and J. S. Chung, *J. Mater. Chem.*, 2011, **21**, 3371–3377.

39 T. Szabó, O. Berkesi, P. Forgó, K. Josepovits, Y. Sanakis, D. Petridis and I. Dékány, *Chem. Mater.*, 2006, **18**, 2740–2749.

40 T. Fernandes, S. F. Soares, T. Trindade and A. L. Daniel-da-Silva, *Nanomaterials*, 2017, **7**, 68.

41 J. Prado-Fernández, J. A. Rodríguez-Vázquez, E. Tojo and J. M. Andrade, *Anal. Chim. Acta*, 2003, **480**, 23–37.

42 A. L. Daniel-Da-Silva, A. M. Salgueiro and T. Trindade, *Gold Bull.*, 2013, **46**, 25–33.

43 S. S. Silva, R. A. S. Ferreira, L. Fu, D. Carlos, F. Mano and L. Reis, *J. Mater. Chem.*, 2005, **15**, 3952–3961.

44 A. L. Daniel-da-silva, J. C. M. Bordado and J. M. Martín-Martínez, *J. Appl. Polym. Sci.*, 2008, **107**, 700–709.

45 R. Oliveira-Silva, J. P. Da Costa, R. Vitorino and A. L. Daniel-Da-Silva, *J. Mater. Chem. B*, 2015, **3**, 238–249.

46 S. F. Soares, T. R. Simões, M. António, T. Trindade and A. L. Daniel-da-Silva, *Chem. Eng. J.*, 2016, **302**, 560–569.

47 M. S. Dresselhaus, A. Jorio, M. Hofmann, G. Dresselhaus and R. Saito, *Nano Lett.*, 2010, **10**, 751–758.

48 F. T. Johra, J. Lee and W. Jung, *J. Ind. Eng. Chem.*, 2014, **20**, 2883–2887.

49 S. Gayathri, P. Jayabal, M. Kottaisamy and V. Ramakrishnan, *AIP Adv.*, , DOI:10.1063/1.4866595.

50 J. Bin Wu, M. L. Lin, X. Cong, H. N. Liu and P. H. Tan, *Chem. Soc. Rev.*, 2018, **47**, 1822–1873.

51 D. López-Díaz, M. López Holgado, J. L. García-Fierro and M. M. Velázquez, *J. Phys. Chem. C*, 2017, **121**, 20489–20497.

52 A. Kaniyoor and S. Ramaprabhu, *AIP Adv.*, , DOI:10.1063/1.4756995.

53 L. Pereira, A. M. Amado, A. T. Critchley, F. Van De Velde and P. J. A. Ribeiro-claro, *Food Hydrocoll.*, 2009, **23**, 1903–1909.

54 R. Dronov, A. Jane, J. G. Shapter, A. Hodges and N. H. Voelcker, *Nanoscale*, 2011, **3**, 3109–3114.

55 S. Eigler, C. Dotzer, F. Hof, W. Bauer and A. Hirsch, *Chem. - A Eur. J.*, 2013, **19**, 9490–9496.

56 J. D. Clogston and A. K. Patri, in *Characterization of Nanoparticles Intended for Drug Delivery.*, ed. S. E. McNeil, Humana Press, 2011, pp. 63–70.

57 B. H. Hameed and M. I. El-Khaiary, *J. Hazard. Mater.*, 2008, **159**, 574–579.

58 D. Kumar and J. P. Gaur, *Bioresour. Technol.*, 2011, **102**, 633–640.

59 A. E. Ofomaja, *Bioresour. Technol.*, 2010, **101**, 5868–5876.

60 H. N. Tran, S. J. You, A. Hosseini-Bandegharaei and H. P. Chao, *Water Res.*, 2017, **120**, 88–116.

61 Y. Xiao, J. Azaiez and J. M. Hill, *Ind. Eng. Chem. Res.*, 2018, **57**, 2705–2709.

62 J. P. Simonin, *Chem. Eng. J.*, 2016, **300**, 254–263.

63 E. C. Lima, A. Hosseini-Bandegharaei, J. C. Moreno-Piraján and I. Anastopoulos, *J. Mol. Liq.*, 2019, **273**, 425–434.

64 M. Muqeet, A. Khalique, U. A. Qureshi, R. B. Mahar, F. Ahmed, Z. Khatri, I. S. Kim and K. M. Brohi, *Cellulose*, 2018, **25**, 5985–5997.

65 R. R. C. Lima, P. D. S. De Lima, V. R. Greati, P. B. F. De Sousa and G. V. S. Medeiros, *Ind. Eng. Chem. Res.*, 2019, **58**, 9380–9389.

Journal Pre-proof

66 A. L. Daniel-da-Silva, T. Trindade, B. J. Goodfellow, B. F. O. Costa, R. N. Correia and A. M. Gil, *Biomacromolecules*, 2007, **8**, 2350–2357.

67 C. Qin, R. Wang and W. Ma, *Desalination*, 2010, **259**, 156–160.

68 D. Quality, *pH Drink.*, 1996, **2**, 7.

Journal Pre-proof

Graphical abstract

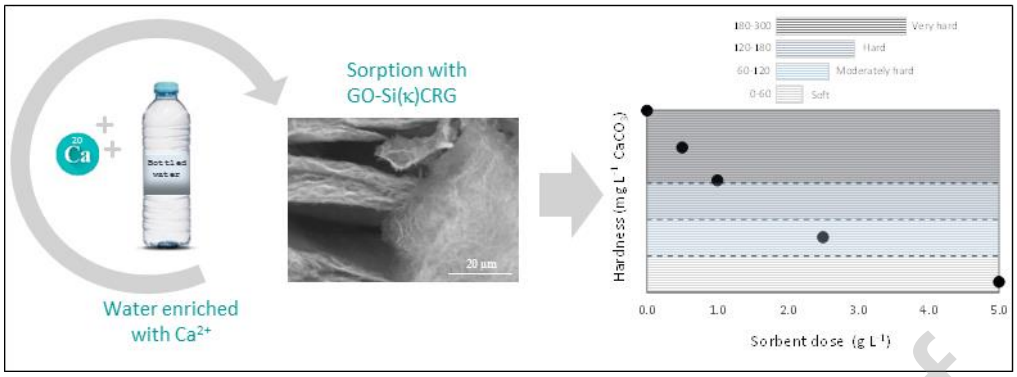

Journal Pre-proof

Credit Author Statement

Conceptualization, L. S. R., A.L.D.-d.-S., P. M., E. P., T.T.; Validation, A.L.D.-d.-S., P. M., E. P and T.T.; Investigation, L.S.R., J.N., S. F.; Writing–Original Draft Preparation, L. S. R., J. N., A.L.D.-d.-S. and S. F.; Writing–Review and Editing, L. S. R., J. N., A.L.D.-d.-S., P. M., S. F., E. P., T. T. ; Supervision, A.L.D.-d.-S., P. M., E. P., T.T.; All the authors contributed to the discussion and reviewed the manuscript.

Journal Pre-proof

Declaration of interests

☒ The authors declare that they have no known competing financial interests or personal relationships that could have appeared to influence the work reported in this paper.

☐The authors declare the following financial interests/personal relationships which may be considered as potential competing interests:

Journal Pre-proof

HIGHLIGHTS

- The surface modification of GO with κ-carrageenan polysaccharide is described
- The water softening performance of GO-based materials was investigated
- The Ca^{2+} removal from water greatly improved by surface modification
- The hybrid GO-Si(κ)CRG was effective in converting very hard water to soft water

Journal Pre-proof